Journal of Mechanics Engineering and Automation 7 (2017) 221-234
doi: 10.17265/2159-5275/2017.04.006

An Investigation of Innovative Experimental and Numerical Techniques to Detect Boundary Layer Transition

Alessandro Cinciripini[2], Pascal Bader[1], Giacomo Persico[2] and Wolfgang Sanz[1]

1. Institute for Thermal Turbomachinery and Machine Dynamics, Graz University of Technology, Graz 8010, Austria

2. Dipartimento di Energia, Politecnico di Milano, Milano 20158, Italy

Abstract: Different methods to detect boundary layer transition are investigated within the scope of this paper. Laminar and turbulent boundary layers exhibit a significantly different behavior, not only regarding skin friction but also for heat-transfer which affects the blade cooling design. The present work presents a novel and non-intrusive measurement technique to detect the transition, based on acoustic concepts. The reliability of the technique was investigated by means of boundary layer measurements over a flat plate in subsonic flow conditions. After a preliminary assessment with a conventional Preston tube, a row of microphones were installed along the plate to correlate transition pressure fluctuations. To provide a comprehensive representation of the experiment, dedicated measurements with a fast response aerodynamic pressure probe were performed to determine the turbulence intensity and the dissipation rate upstream of the flat plate. The experimental results were systematically compared with calculations performed with three different computational fluid dynamics solvers (ANSYS-Fluent®, ANSYS-CFX®, OpenFOAM®) and using both the k-k_l-ω and the γ-Re_θ transition models. Results show a fair agreement between CFD (computational fluid dynamics) predictions and the acoustic technique, suggesting that this latter might represent an interesting alternative option for transition measurements.

Key words: Boundary layer transition, acoustic measurements, CFD, Preston tube, flat plate.

Nomenclature

c_f	Skin-friction coefficient
f	Frequency
k	Turbulent kinetic energy
k_L	Laminar kinetic energy
M	Mach number
p	Static pressure
p_t	Total pressure
q_{probe}	Local dynamic pressure
q_∞	Free-stream dynamic pressure
Re	Reynolds number
Tu	Turbulence intensity
u	Local stream-wise velocity
U	Local free-stream velocity
x	Streamwise coordinate
y	Distance to the wall
y^+	Dimensionless wall distance
δ_{99}	Boundary layer thickness
γ	Intermittency
ϵ	Turbulence dissipation rate
θ	Momentum thickness
ρ	Density
τ	Time period
τ_0	Wall shear stress
τ_I	Integral time scale

Corresponding author: Dipl.-Ing. Dr. techn. Pascal Bader, B.Sc., research assistant, research fields: CFD and non-invasive measurement techniques.

1. Introduction

Transition is the process by which a laminar flow becomes turbulent. A laminar flow is characterized by a well ordered particle motion opposed to a turbulent one, where the paths of the particles appear chaotic. Transition is a very complex process, not yet fully understood, and its prediction is nowadays still subject of an intensive research. It occurs in most of turbomachinery and aeronautics applications, such as gas turbines, compressors, turbofan engines or plane wings.

The boundary layer is the small zone between the wall and the free-stream where viscous effects are relevant. In spite of its small size, the boundary layer is crucial because it determines the skin friction and the heat transfer between flow and solid surfaces. A boundary layer can present either a laminar or a turbulent nature, which affects substantially the skin friction and the heat transfer rate, due to a different velocity gradient at the wall. A turbulent boundary layer presents a higher skin friction indeed. Also the heat transfer through solid surfaces increases considerably in a turbulent boundary layer. Depending on the application, this issue can be problematic, since overheating can take place. For these reasons, predicting where transition develops is crucial, not only from the economical point of view, but for safety reasons too. Moreover, a turbulent boundary layer presents a much more stable behavior, which means that flow separation (stall) occurs less often, in contrast to a more unstable behavior of a laminar boundary layer.

When a fluid flows past a stationary solid surface, a laminar boundary layer develops, growing from the leading edge. During its interaction with the solid structure, the boundary layer may become turbulent. This process passes through several stages within the transitional zone, until it reaches a fully turbulent behavior. The transition position and the length of this process are affected by many parameters like free-stream velocity, acceleration, free-stream turbulence etc. The comprehension of the physical principles underlying these features would be instrumental for controlling the boundary layer state, leading to an improvement in cascade efficiency and, eventually, in engine performance.

In 1991, Mayle [1] published one of the most important overviews about boundary layer transition. He gathered and analyzed the main results of available previous experiments, in order to identify the influence on transition of several flow parameters. Additional experiments were performed in the last years by different research groups. Yip et al. [2] carried out in-flight measurements with a Preston tube. They detected the boundary layer transition over the wing surfaces and analyzed the influence of the flight conditions on the boundary layer behavior. Oyewola et al. [3] showed how to measure the turbulence generated within boundary layers with the help of hot-wire probes and LDV (laser-doppler velocimetry). In 2008 Døssing [4] showed the results of acoustic measurements performed on an airfoil with the aim of detecting the boundary layer transition. More recently, hot-film measurements were performed, e.g., by Mukund et al. [5], Preston tube and thermographic measurements by Bader and Sanz [6]. Recently, Bader et al. [7] used LIV (laser interferometric vibrometry) to identify the transition.

Beside experimental research, specific turbulence models have been recently developed with the scope of predicting the transition process in the framework of CFD (computational fluid dynamics) solvers. Among the most important transitional models the k-k_l-ω [8] and γ-Re_θ [9] can be listed. Both are based on the k-ω model [10], with the addition of one or more equations that model the transition process.

The aim of this work is to test an innovative acoustic measuring technique, which is supposed to be able to detect the boundary layer transition over a zero pressure gradient flat plate and compare these results to both Preston tube measurements of the same flow and to CFD simulations of the experimental case, which were carried out to verify the effectiveness of the transitional models employed. This paper is structured as follows: at first the experimental set-up and the numerical model are described, then the turbulence and transitions measurement are presented. Finally the comparison with the numerical simulations is reported.

2. Experimental Setup

The experiments reported in this paper were performed at ITTM (the Institute for Thermal

Turbomachinery and Machine Dynamics) in Graz University of Technology, Austria. The facility is a continuously operating open-loop wind tunnel. Within the flow channel, about half of its height, a horizontal carbon steel flat plate is positioned. The flat plate entirely fills the transversal width of the inner cross section. The dimension of the channel internal cross-section is 200 × 200 mm^2 and it is 2 m long. Fig. 1a shows the vertical section of the channel.

The air flow is delivered by a centrifugal compressor with a max. power of 125 kW, corresponding to a mass flow rate of approximately 0.8 kg/s. The compressor delivers air into a flow settling chamber. From this chamber the flow is transported via a flow-calming section formed by a diffuser with guiding vanes towards the test area. A schematic drawing of the test bench is given in Fig. 1b. A damping element made of polymeric rubber is inserted between the diffuser and the channel. The flow velocity was measured with the help of a rotating vane anemometer. It is equal to 18.12 m/s.

The flat plate is inclined about 1.3° to the mean stream vector. As reported in Ref. [11], a very small inclination of the plate ensures an attached flow over it and also a steady leading edge stagnation point. Nevertheless, this solution causes a small pressure gradient over the flat plate, consequently a flow acceleration over it. According to Mayle [1], for low turbulence levels the effect of acceleration is significant, while for high levels it is negligible. Therefore, at the high levels of turbulence found in gas turbines, the onset of transition is primarily controlled by the free-stream turbulence intensity. As reported afterwards, a high turbulence level (Tu > 5%) is found in the test bench flow, then, according to Mayle [1], the effect of this acceleration is considered negligib (see Fig. 2).

Every experimental measurement was performed in thermal steady-state conditions.

3. Numerical Models

The computational domain shown in Fig. 2 represents the entire channel section. The mesh was built 2-dimensional, so it was assumed that the external boundary layers in span-wise direction do not affect the channel midsection where the experimental investigations were carried out. Three grids with different cell density were built in order to perform a mesh independence analysis. The coarsest one has about 70 k cells, the medium one about 192 k cells, while the finest one about 507 k cells. Fig. 3 shows the coarse mesh. Near the plate the mesh was built with

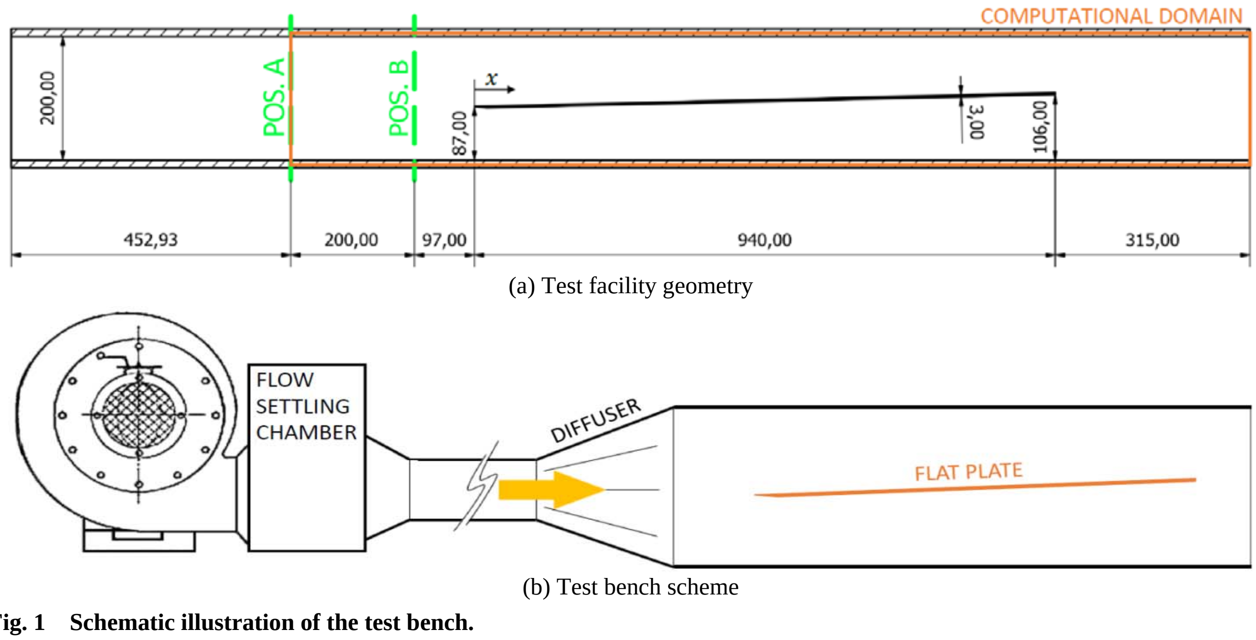

Fig. 1 Schematic illustration of the test bench.

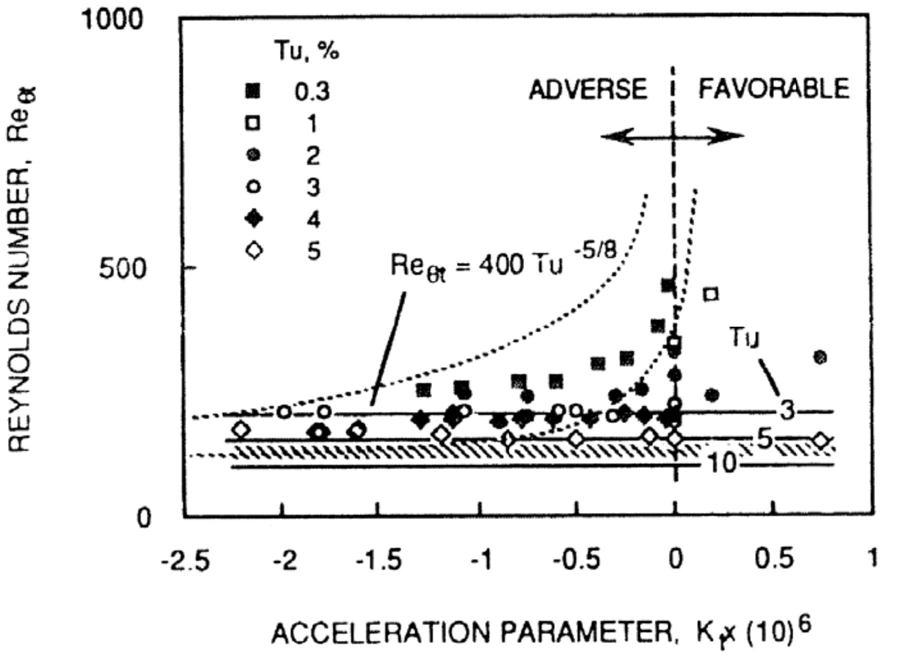

Fig. 2 Flow acceleration versus transition position.

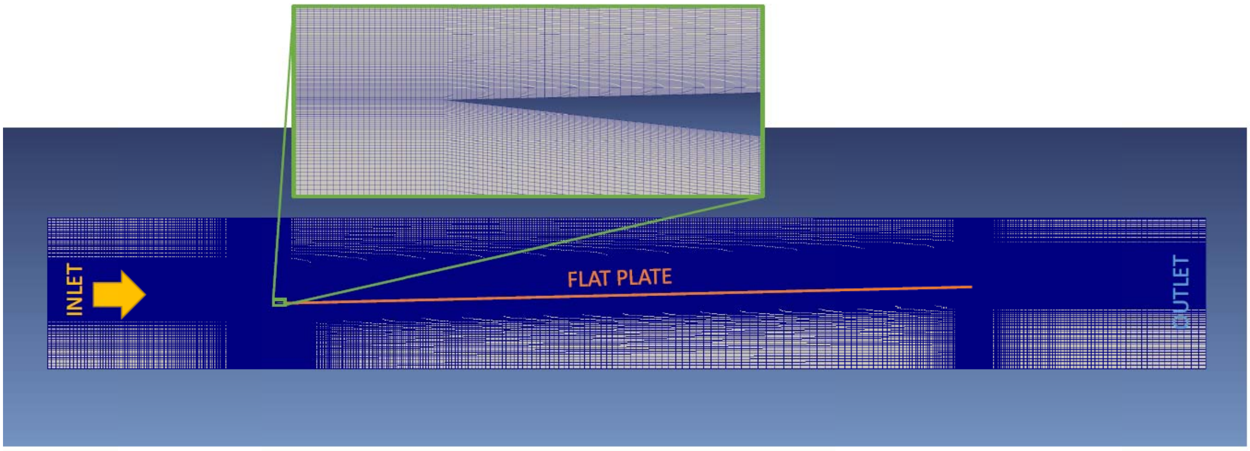

Fig. 3 Computational domain.

a refinement, in order to ensure a y^+ sufficiently small for reliable results. For all the three meshes y^+ was verified that remains below 1 along the plate.

Regarding the boundary conditions, the inlet velocity is taken from the measurements with a rotating vane anemometer and the values of the turbulent kinetic energy and the turbulence dissipation rate are obtained from FRAPP measurements, which are described in the following section. At every wall a no-slip velocity condition is set, but at the upper and the lower walls of the channel a wall-function for the turbulence models is activated, in order to save computational time.

ANSYS-Fluent® and ANSYS-CFX® in addition to the open-source code OpenFOAM® were employed. While ANSYS-Fluent® and OpenFOAM® solve the flow equation using the segregated SIMPLE algorithm, which is more robust and provides a lower computational cost, ANSYS-CFX® makes use of a fully-coupled solver.

Every code solves the Navier-Stokes equations with the RANS hypothesis, for incompressible flow (the flow velocities are much lower than Ma = 0.3) and assuming a steady-state.

The simulations performed with OpenFOAM® were run employing both the the k-k_l-ω and γ-Re_θ transitional models. ANSYS-CFX® was run with the γ-Re_θ model, while ANSYS-Fluent® simulations were performed with the k-k_l-ω model. Hence, 4 different types of numerical simulations for the BL transition were analyzed and are presented in the following.

4. Turbulence and Dissipation Measurements

As well known in Ref. [1], the boundary layer transition is strongly affected by the turbulence level of the flow. Therefore, in order to carry out a proper technical analysis of transition, a direct measurement is crucial, also to supply with proper boundary conditions the numerical simulations performed in this work. In order to obtain the turbulence quantities, a cylindrical single-sensor FRAPP (fast response aerodynamic pressure probe) is employed. A miniaturized piezo-resistive pressure sensor (Kulite XCE-062, uncertainy +/- 80 Pa) is installed inside the probe head, which has an outer diameter of 1.85 mm. The FRAPP, here used for time-resolved total-pressure measurements, has a promptness of about 80 kHz. Full details on the probe design and static, dynamic and aerodynamic calibration can be found in Ref. [12].

The measurements were carried out downstream of the diffuser (Position A in Fig. 1b), in correspondence with the numerical domain inlet. Close to the leading edge (Position B) Tu is measured again to obtain the turbulence dissipation and the turbulence length scale, respectively. In both positions the measurements were carried out in seven different channel heights, so every 25 mm from the top to the bottom, in order to obtain a mean value of Tu along the channel cross-section. The signals were acquired consecutively in every location for 5 seconds.

The FRAPP provides an instantaneous total pressure signal, from which the flow fluctuations intensity can be obtained. According to the Reynolds decomposition technique, every stationary fluid-dynamic quantity can be split into two components, i.e., the ensemble average and fluctuating parts of the quantity. Being the flow statistically stationary in the present configuration, the ensemble average coincides with the time-average. This decomposition technique can be applied both to the time-varying pressure and to the time-varying velocity. According to Camp and Shin [13], the definition of turbulence intensity Tu of a flow is given by:

$$Tu = \frac{u'_{rms}}{\bar{u}} = \frac{1}{\bar{u}} \cdot \sqrt{\frac{1}{N}\sum_{i=1}^{N} u_i^2(t)} \tag{1}$$

where, N is the number of samples of the time-signal, $\bar{u}$ and $u_i(t)$ represent the average and the fluctuating components of the flow velocity respectively, and u'_{rms} the root mean square of u_i. In order to relate the total pressure fluctuations that are measured by the FRAPP probe to the velocity fluctuations, Persico et al. [14] provided the following formula, based on an approach by Ref. [15]:

$$\begin{aligned} {p'_{t,rms}}^2 = 0.49\,\rho^2(1-0.175\,Ma)^4 {u'_{rms}}^4 \\ + \rho^2\bar{u}^2(1 \\ + 0.5\,Ma^2){u'_{rms}}^2 \end{aligned} \tag{2}$$

where, $p'_{t,rms}$ is the RMS value of the fluctuating total pressure, Ma is the Mach number of the free-stream and ρ the fluid density. Working out this equation, u'_{rms} is obtained.

Before calculating $p'_{t,rms}$ from the data, it is necessary to remove all the periodic components of the measured raw signal, if any, since only the non-periodic stochastic part of the signal represents turbulence [16]. These periodic components are the blades passing frequencies or flow fluctuations due to the rotor-stator interaction inside the centrifugal compressor. To perform this reduction, the acquired signal has to be FFT (Fast Fourier Transformed) in order to “chop” these frequency components, resulting in a spectrum where the peaks are replaced with averaged data from near frequencies. The phases of the signals, needed afterwards to perform the inverse FFT, were worked out accordingly. This procedure is explained in details in Ref. [13]. High- and low-pass filters have to be also applied at the frequency-transformed signal, in order to discard frequency ranges not related to turbulence. After that, every processed signal is transformed back into a time-signal, by means of an IFFT (inverse Fast Fourier Transform) algorithm, so that the RMS value of the velocity fluctuations can be evaluated.

Fig. 4 shows an unchopped signal spectrum, measured with FRAPP. The green arrows point out the deterministic periodic components that have to be chopped. The main periodic component can be seen on the left, followed by the harmonics for higher frequencies. In this figure, also the Kolmogorov -5/3 energy cascade function is plotted. It can be observed that the spectrum fits the -5/3 up to about 7 kHz. Here, the low-pass filter is applied. However, the choice of the frequency in which this filter is applied does not affect considerably the final results, since little energy is transported by the flow in the high frequency range.

In order to obtain the high-pass filter frequency, the integral length scale has to be estimated. The integral length scale L assigns a spatial dimension to the turbulent structures and can be identified as the average size of the largest eddies involved in a flow. Once the average size of these turbulence structures is known, their characteristic time scale τ_I, which corresponds to the high-pass frequency, can be estimated. Considering that u'_{rms} represents the characteristic velocity of the flow fluctuations, it may be assumed as the rotational velocity of the highest scale eddies: $\tau_I \cong L/u'_{rms}$. Thus, the inverse of τ_I corresponds to the high-pass frequency f_I. According to Camp and Shin [13], the integral length scale can be computed by means of an autocorrelation function $ACF(\tau)$ of the turbulent velocity time-signal, which reads:

$$L = \bar{u} \int_0^{\infty} ACF(\tau) d\tau \qquad (3)$$

This definition is effective only if every deterministic periodic component of the signal, such as the blade passing frequencies of the compressor, is removed. Moreover, this calculation is applied until the first zero-crossing point (so assuming that the integral from first zero-crossing to infinite is null), since the infinite limit is not applicable. The estimate is performed with the processed time-signal, so, after the analysis in the frequency domain explained above and the IFFT applied. Nevertheless, both L and u'_{rms} at the first computation are based on a signal where no high-pass filter is applied, since this frequency is still unknown. Thus, an iterative procedure is required: after the first computation, f_I is applied to the Fourier transformed signal in order to cut out the low frequency range that is not related to turbulence. The IFFT is then computed and this procedure repeated with the new u'_{rms} and the new L. The iterations are repeated until convergence is obtained. It succeeds rapidly after a mean of 8 computations for the different

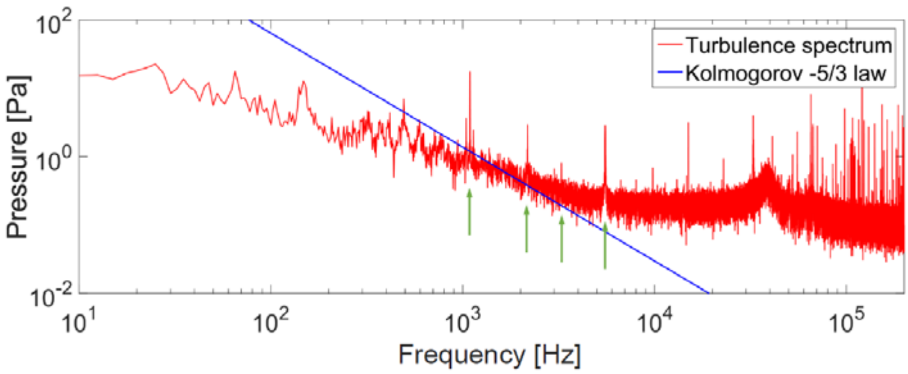

Fig. 4 Measured FRAPP uncut signal.

Table 1 Turbulence quantities.

	Position A	Position B
u'_{rms}	1.230 m/s	1.165 m/s
k	2.269 m²/s³	2.036 m²/s³
Tu	6.788%	6.429%
L	0.0025 m	
f_I	320 Hz	
ϵ	21.11 m²/s³	

positions. Table 1 shows the results of the turbulence quantities, as averaged values of different measuring locations along the cross-section, in both Pos. A and Pos. B.

In order to simulate the experimental investigations with CFD the dissipation rate is required alongside the turbulence intensity. Therefore, an approach suggested by Bader and Sanz [6] was used. Basically the approach adopts the averaged turbulence levels that, as discussed before, were calculated in two different positions (A and B). Using these values, ϵ can be calculated directly. The transport equation for the turbulent kinetic energy k, with the assumption of steady-state and non-accelerating flow, isotropic turbulence and with no turbulence production between the two measured positions reduces to [17]:

$$\epsilon = -\bar{u}\frac{dk}{dx} \tag{4}$$

According to Schlichting and Gersten [18], at a certain distance from screens or honeycombs, the turbulence in a wind tunnel becomes isotropic. Therefore, the turbulent kinetic energy k can be computed in both measuring positions by means of u'_{rms}:

$$k = \frac{3}{2}(u'_{rms})^2 \tag{5}$$

Since the distance between these two measurement positions is known together with k of these positions, ϵ can be estimated by using Eq. (5), assuming a linear decay. The results of these evaluations are given in Table 1. The values related to Position A of the test facility, which corresponds to the inlet of the computational domain, were used as boundary conditions for the numerical simulations.

According to Mayle [1], due to the high turbulence level observed, a bypass type transition occurs over the flat plate. In this condition there is no development of Tollmien-Schlichting waves because they occur only in a natural transition, so when the turbulence intensity of the free-stream is very low. For this reason, a frequency analysis of the spectrum as well as of the scales of the Tollmien-Schlichting waves cannot be performed.

5. Transition Measurements

In this section, the experimental investigations that were carried out to detect the boundary layer transition are discussed. First, the Preston tube measurements are presented, followed by the acoustic measurements.

5.1 Preston Tube Measurements

Turbulent and laminar boundary layers present different velocity profiles $u(y)$ at the walls. A turbulent boundary layer is characterized by a high exchange of momentum in transverse direction, causing a more uniform distribution over the cross-section of a duct, if compared to a laminar boundary layer. The Preston tube measuring method employs this different physical behavior to detect the boundary layer transition.

Along the flat plate surface, several static pressure tappings were embedded into the plate. The diameter of the tappings is 0.5 mm and they are equally spaced with 50 mm, resulting in 18 static pressure tappings along the plate.

A Preston tube was traversed all over the plate in the stream-wise direction in order to capture the stagnation pressure of the flow. The probe consists of a Pitot tube with an outer diameter of 1 mm and an inner diameter of 0.5 mm, which is the same dimension as the tappings. Fig. 5 shows these probes. Considering the size of the tube section, it allows to measure the flow velocity at $y_1 = 0.5$ mm from the wall. The measurements were performed moving the Preston tube step-by-step from the leading edge toward the trailing edge of the plate, in every position.

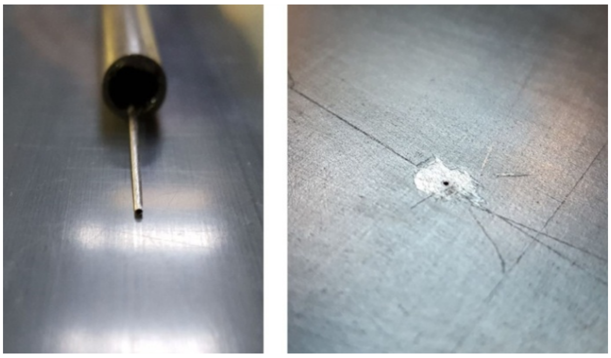

Fig. 5 Preston tube and static pressure tappings.

The acquisition system can provide up to 2 Hz sample rate, due to the speed of sound lag. For this reason, steady-state measurements (non-time-depending) were executed.

The data were acquired for several seconds in order to calculate a mean value of pressure, for each position. The total pressure that the Preston tube measures were then used, together with the static pressure measurements, to calculate the non-dimensional dynamic pressure. Let q and q_1 be the local and the free-stream dynamic pressure respectively, Fig. 6 shows the working principle of this probe. The ratio q/q_1 is the non-dimensional dynamic pressure and it is a good parameter to visualize the boundary layer transition. According to the theoretical principle, the graph shows a sudden increase of q/q_1 in the transition region. It confirms the fact that more energy is transported normal to the stream-wise direction toward the wall, in a turbulent boundary layer.

Let x be the distance from the leading edge, according to Bader and Sanz [6] the non-dimensional dynamic pressure is given by:

$$\frac{q_{probe}}{q_\infty} = \frac{p_{t,probe}(x) - p(x)}{p_{t,\infty} - p(x)} \tag{6}$$

where, p_t and p are the total pressure and the static pressure respectively, and $q_\infty = q_1$. Before performing the measurements, the Preston tube size has to be validated: the distance between the probe middle axis and the wall y_1 has to be at least half of the boundary layer thickness, in every measuring position. The first measuring position (50 mm from the leading edge) is the most critical one—assuming that the transition occurs after this point—since the laminar boundary layer has just started to develop. The Blasius solution was employed to estimate the boundary layer thickness $\delta_{99} = 4.9\, x\, (Re_x)^{-0.5}$ at 50 mm from the leading edge, based on the local free-stream velocity. The formula provides a thickness of 1.16 mm, confirming the minimum thickness as it is greater than twice y_1.

Fig. 7 shows the non-dimensional dynamic pressure from the leading to the trailing edge of the plate. The onset of transition can be seen at about 150/200 mm, after which the dynamic pressure suddenly changes from 0.4 to 0.8 of the free-stream value. This phenomenon indicates that the velocity profile changes from laminar to turbulent, where the momentum exchange is enhanced toward the wall. Employing a distance of the transition onset equal to 175 mm, the critical Reynolds number is $Re_{x,crit} = 1.82 \times 10^5$. Schlichting and Gersten [18] experimented that the range of Re_x in which the onset transition occurs is between 3.5×10^5 and 10^6

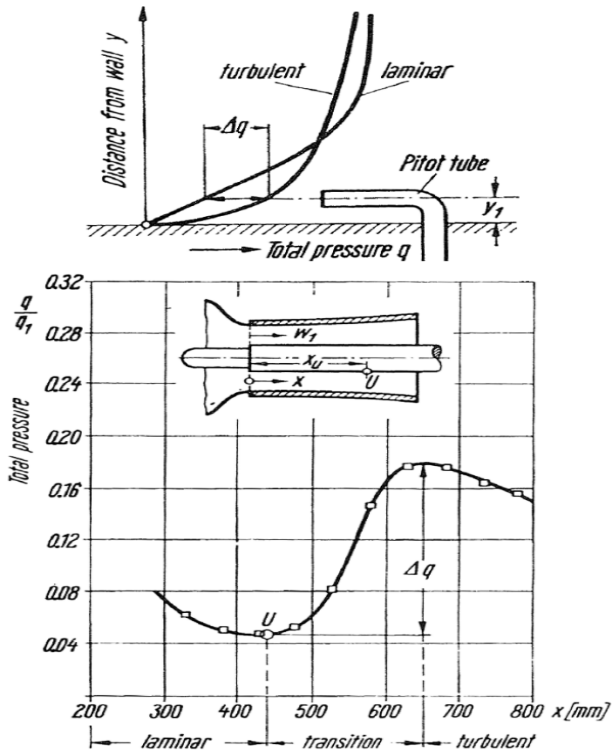

Fig. 6 Explanation of the Preston tube measurement theory [18].

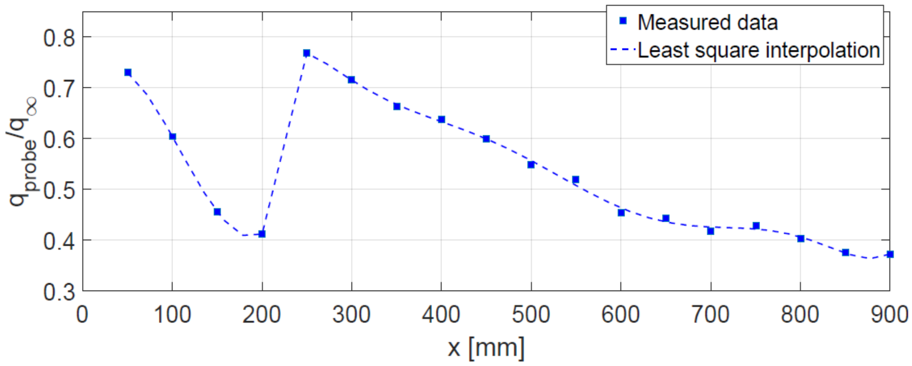

Fig. 7 Non-dimensional dynamic pressure.

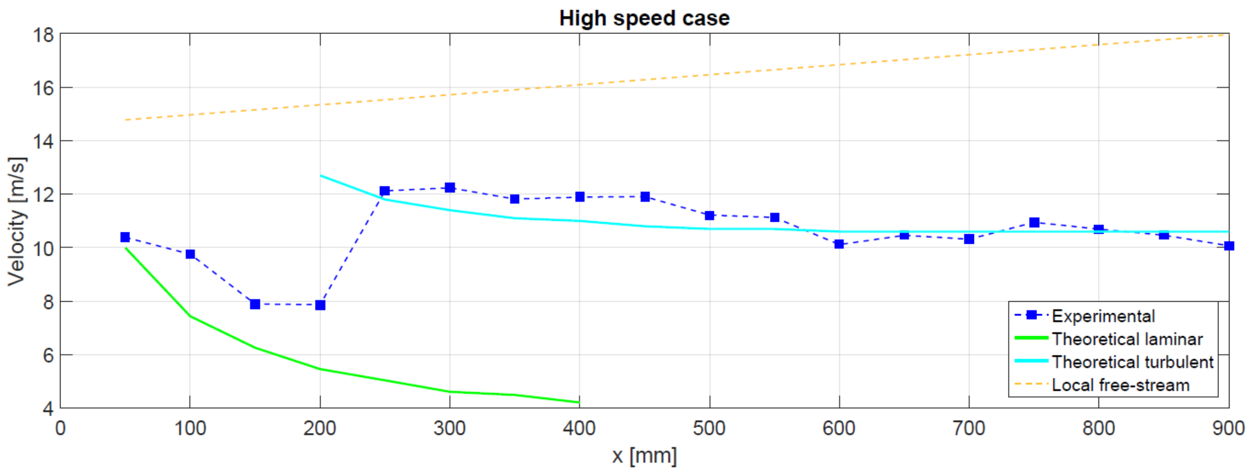

Fig. 8 Theoretical/experimental boundary layer velocity comparison.

for streams with low levels of turbulence ($Tu \cong 0.5$). In this case the value found is out of range because of the high turbulence level. At about x = 300 mm the transition process is supposed to be completed.

In order to identify the laminar and turbulent BL along the flat plate, a comparison with the classical boundary layer solutions is performed. The aim of this operation is to match the velocities measured experimentally by the Preston tube—that can be computed from the dynamic pressure—with the theoretical velocities. The theoretical velocities along a no pressure gradient flat plate are obtained by means of the Blasius solution, for laminar BL, and by means of the 1/7 power law for the turbulent BL [18]. The velocity profiles that these theories provide, are evaluated at the distance from the wall where the Preston tube measures the kinetic head (0.5 mm). The 1/7 power law is defined as:

$$\frac{u}{u_\infty} = \left(\frac{y}{\delta_{99}}\right)^{1/7} \tag{7}$$

Fig. 8 shows that the theoretical laminar and turbulent velocity profiles $u(y)$, evaluated at 0.5 mm from the wall, fit very well the experimental results shown above. It can be seen that at about 150 mm from the leading edge the experimental curve detaches from the theoretical solution to reach the turbulent profile.

5.2 Acoustic Measurements

Acoustic measurements were performed with high frequency response microphones on the flat plate, with the scope to detect boundary layer transition. Several microphones were embedded into the structure of the flat plate, below the surface. The microphones do not generate a blockage effect, making this measurement method non-intrusive. They can measure the sound pressure level of the boundary layer through a series of thin holes aligned, with a diameter of 1 mm and a depth of 1 mm, which were drilled over the surface. The signals are then recorded simultaneously, monitoring the variation of the static pressure fluctuations along the plate.

The detection of the transition location is based on an evaluation of the RMS pressure fluctuations, registered by the microphones along the plate. The transition from laminar to turbulent boundary layer is associated with a large increase in velocity fluctuations, due to the nature of the turbulent boundary layer. The velocity fluctuations are coupled to the pressure fluctuations, as it can be seen by analyzing the Navier-Stokes equation, after the divergence operator is applied. By assuming an incompressible, two-dimensional, inviscid and steady-state flow, the result is a relationship between pressure and velocity. The equation takes the form:

$$\frac{1}{\rho}\nabla^2 p = -\frac{\partial u_i}{\partial x_j}\frac{\partial u_j}{\partial x_i} \tag{8}$$

Farabee [19] took this equation to perform a Reynolds decomposition into mean and unsteady terms. Splitting each quantity and then subtracting the time-averaged equation yields to:

$$\frac{1}{\rho}\nabla^2 p' = -2\frac{\partial \bar{u}_i}{\partial x_j}\frac{\partial u'_j}{\partial x_i} - \frac{\partial^2 (u'_i u'_j - \overline{u'_i u'_j})}{\partial x_j \partial x_i} \tag{9}$$

Eq. (9) is a Poisson equation for the fluctuating pressure p in a turbulent flow. The source terms on the right hand side of Eq. (9) represent the MT (mean-shear-turbulence) interaction (first term) and the TT (turbulence-turbulence) interaction (second term) [19]. This relationship suggests that, in a turbulent flow, the pressure fluctuations are a result of the velocity fluctuations and their gradients.

A number of 24 microphones were used for this experimental investigation. The model is the 40 BD "1/4" Pre-polarized Pressure Microphone by G.R.A.S.®, operating with a high-precision condenser technology. Their precision respects the IEC 61094-4 requirements. They provide a flat frequency response, from 4 to 70,000 Hz with +/- 2 dB of distortion, and from 10 to 25,000 Hz with +/- 1 dB of distortion. Their low sensitivity (equal to 1.6 mV/Pa) makes them ideal for sound measurements at high sound pressure levels, up to 174 dB and a dynamic range of 166 dB. The microphones signal is processed by the pre-amplifier G.R.A.S.® 12 AN and digitalized by the ADC PXI-4496 by National-Instruments®. The shape of these microphones is cylindrical, the diameter is about 6 mm and they are 50 mm long. The head presents a diaphragm that transmits the sound vibrations to the condenser.

A data processing equal to that done for the FRAPP measurements (Section 4) has to be performed in order to chop the deterministic components related to blade passing frequencies and the ranges of the spectrum that do not belong to turbulence. For this reason, due to the presence of high amplitude deterministic components, a direct comparison between raw time signals cannot be carried out. After the frequency-domain analysis, the IFFT is applied to each signal in order to obtain the RMS value of the pressure fluctuations. The first experimental results showed that the microphones were measuring the modes of vibration of the flat plate. Most of the sound pressure level that each microphone was registering actually came from the flat plate vibration, which dominated over the relatively low "noise" caused by aero-acoustics of turbulence.

In order to overcome this problem, a turbulator 1 mm thick was mounted very close to the leading edge of the plate generating a turbulent boundary layer. If the turbulator is very thin, the dead-water region downstream is small too. The aim of this action is to create an experimental set that could be used as a fully turbulent reference case. CFD simulations with OpenFOAM® were performed in order to estimate the length of dead-water region downstream the turbulator. It was seen that the flow reattached over the flat plate before the first measurement position.

The final result is obtained by dividing the RMS pressure value calculated in each measuring point without the turbulator by the corresponding value of the fully turbulent case. Theoretically, the resulting values should be equal to 1 in the locations where both cases are turbulent, between 0 and 1 where the transitional case has a laminar boundary layer.

Fig. 9 shows the graph of the non-dimensional p_{rms}, i.e., the RMS pressure values made non-dimensional using the reference turbulent case. The values close to the leading edge are lower than 1, according to what was stated before. Starting from the value at 50 mm from the leading edge, the graph increases until it reaches a peak. After that, a moderate decrease takes place, reaching a constant overall trend. The peak agrees with the theory because Eq. (8) shows that the pressure fluctuations are the result of velocity fluctuations and their gradient. Within a transitional boundary layer, the pressure fluctuations arise from the point where small turbulent spots are formed to a fully developed turbulent boundary layer, so the sound pressure level measured by the microphones is expected to reach a peak amplitude in the transitional region. A peak of pressure fluctuations in transitional boundary layers was also shown by Døssing [4] and Barrett [20]. In these works they both established that a peak of RMS pressure was registered with acoustic measurements.

Furthermore, the location where the graph reaches the peak identifies the point of a laminar/turbulent equal distribution within the transitional boundary layer, i.e., the intermittency $\gamma = 0.5$. The intermittency γ, defined in every stream-wise position, identifies the fraction of time in which a boundary layer is turbulent, in the transitional zone. This quantity describes well the transition process because the turbulent spots appear and disappear continuously [21].

6. Comparison between Experimental and Numerical Investigations

In this section, the experimental results are compared with numerical simulations. Concerning the numerical results, in order to see the transition location, the skin friction coefficient c_f is plotted along the flat plate. c_f is a good parameter to point out the transition location, because the wall shear stress varies considerably between a laminar and a turbulent boundary layer. It is defined as:

$$c_f = \frac{\tau_0}{0.5\rho u_\infty^2} \tag{10}$$

where τ_0 is the wall shear. Thus, c_f is proportional to the velocity gradient in the wall-normal direction. u_∞ is the local free-stream velocity. The curves of the skin friction coefficient of laminar and turbulent boundary layers are provided by the Blasius solution and the 1/7 power law respectively (Eq. (7)).

Fig. 10 shows the transition results of both numerical simulations and experimental investigations. In order to make a comparison of the transition location, they are plotted on top of each other. For each type of investigation, the specific physical quantity shows that the transition process is plotted. The transition location is visualized by the point of a laminar/turbulent equal distribution in the transitional

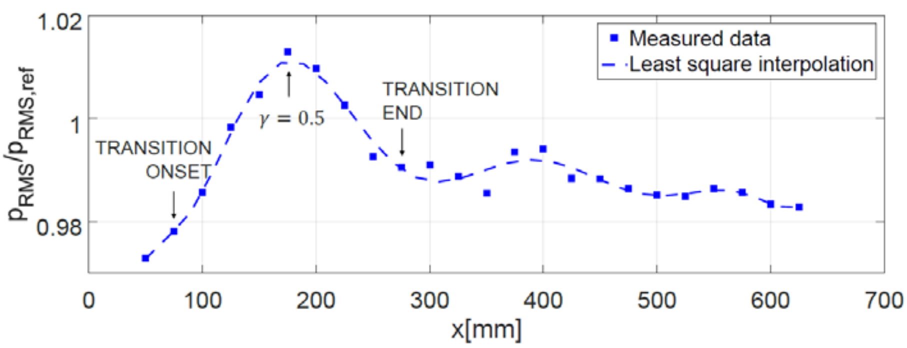

Fig. 9 Non-dimensional RMS pressure data.

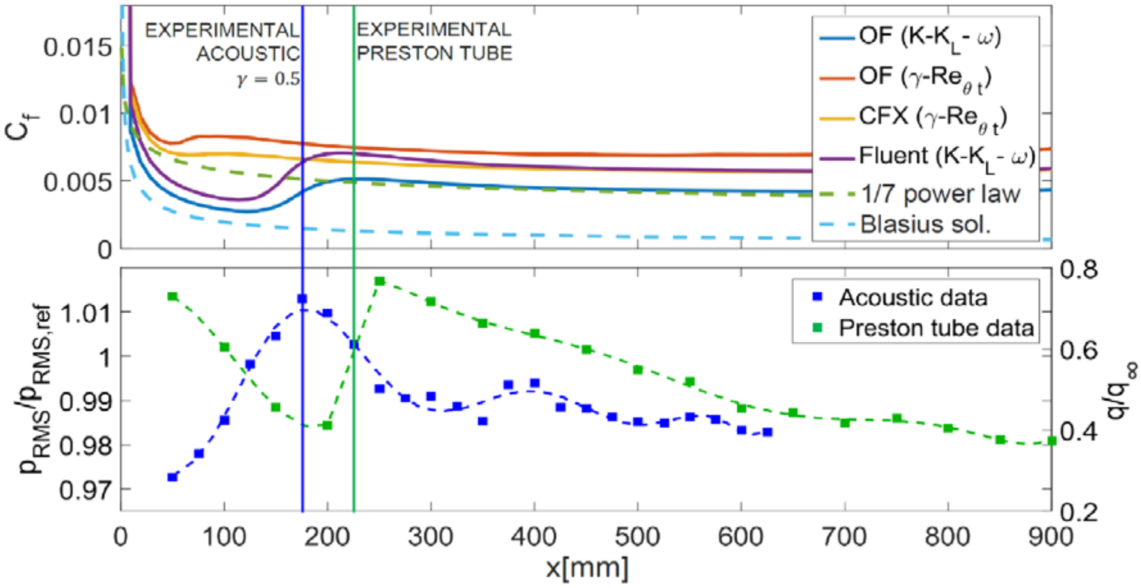

Fig. 10 Comparison between numerical and experimental results.

boundary layer (intermittency $\gamma = 0.5$). This choice is reflected by the fact that the onset transition is hard to identify in the acoustic measurements. For the same reason, the critical Reynolds number will not be considered as a reference point and it will not be computed as well. For the computation results, the location of equal laminar/turbulent distribution is supposed to be in the middle of the stretch where the curve detaches from the laminar level to reach the turbulent one.

The two experimental results agree reasonably well in identifying the transition location. A little difference in the transition location is observed, and it may be due to different environmental conditions when the measurements were carried out and a different roughness of the surface between the experimental investigations. A thin metal plate with the drilled holes had to be placed over the flat plate to perform the acoustic measurements indeed. The experimental results agree very well with the numerical simulations that employ the k-k_l-ω model. Concerning this transitional model, OpenFOAM® and ANSYS-Fluent® present nearly the same transition onset and transition end. Therefore, it can be concluded that assigning the actual turbulence intensity and turbulence dissipation at the inlet, k-k_l-ω is able to properly predict the transition location in a flat plate. It can be seen that the OpenFOAM® k-k_l-ω simulation better fits the turbulent profile provided by the empirical correlation. Considering that the Blasius solution is valid for flows with a very low level of perturbations [8], a reason why the theoretical laminar curve does not fit perfectly the calculated one is the fact that a bypass transition (high free-stream Tu level) occurs here.

Both OpenFOAM® and ANSYS-CFX® fail to predict the measured transition location zone with the γ-Re_θ model. A fully turbulent boundary layer is predicted along almost the total length of the plate. Additional simulations performed with this model showed that the correct transition location is predicted if an inlet Tu of about 3% is set. In this case, the ANSYS-CFX® solution also fits the value of $\boldsymbol{c_f}$ provided by the empirical correlations. This clarifies the sensitivity of numerical models to boundary conditions in predicting the transition, and calls for further development of computational tools and experimental devices to investigate transition.

7. Conclusions

In the present work an investigation on the boundary layer transition over a zero pressure gradient flat plate has been presented, with emphasis on the evaluation of an innovative non-intrusive measuring technique. To this end, experimental investigations and numerical simulations with several codes and models were performed. A direct measurement of the inlet flow turbulence properties was carried out as well, in order to simulate properly the transition phenomenon with the CFD codes.

In the first part of the paper a new experimental technique to study the boundary layer behavior has been presented and assessed. Despite the high intensity vibration of the plate, the acoustic measurements performed by means of condenser microphones were able to detect the transition zone. The transition area fits quite well the one identified by the Preston tube and some CFD simulations. Due to the vibrations of the flat plate that hide the acoustic effects of turbulence, reference measurements were performed with a turbulator. Further investigations have to be performed with lower inlet velocity and turbulence level in order to generate the boundary layer transition more downstream. In this way, the acoustic behavior of the laminar boundary layer can also be explored. In conclusion, the novel measurement technique has been found to detect the boundary layer transition only if the solid body over which this transition occurs has a high stiffness, such as turbine blades or bluff bodies. This non-intrusive technique is very promising because it allows to measure the nature of boundary layers real-time in operating machines, as the microphones can be installed inside the body structure. To reach these results, it is necessary to validate cheap and robust condenser microphones that can be used in industrial applications.

The second important achievement of this work is the very good transition prediction achieved using the CFD codes. A direct measurement of the inlet turbulent properties of the flow is crucial. A specific data-processing procedure was developed to compute the turbulence quantities. OpenFOAM® and ANSYS-Fluent®, implementing the k-k_l-ω model, have been shown to correctly predict the measured transition position, and OpenFOAM® also provided results that match very well the values estimated using classical empirical correlations.

Acknowledgement

The authors gratefully acknowledge financial support from the Austrian Federal Ministry for transport, innovation and technology in funding part of this work by the project RELAM within the Austrian Aeronautics Program TAKE OFF.

The authors would like to especially thank Andreas Marn, Sabine Bauinger, Manuel Laublättner, and the staff of the laboratory of the ITTM for the immense support during the setup of the test bench and the measurement campaign.

References

[1] Mayle, R. E. 1991. "The Role of Laminar-Turbulent Transition in Gas Turbine Engines." *Journal of Turbomachinery* 113 (4): 509-36.

[2] Yip, L. P., Vijgen, P., Hardin, J. D., and Van Dam, C. P. 1993. "In-flight Pressure Distributions and Skin-Friction Measurements on a Subsonic Transport High-Lift Wing Section." AGARD CP-515.

[3] Oyewola, O., Djenidi, L., and Antonia, R. 2003. "Combined Influence of the Reynolds Number and Localised Wall Suction on a Turbulent Boundary Layer." *Experiments in Fluids* 35 (2): 199-206.

[4] Døssing, M. 2008. *High Frequency Microphone Measurements for Transition Detection on Airfoils.* Technical Report, Danmarks Tekniske Universitet, Risø Nationallaboratoriet for Bæredygtig Energi.

[5] Mukund, R., Narasimha, R., Viswanath, P. R., and Crouch, J. D. 2012. "Multiple Laminar-Turbulent Transition Cycles around a Swept Leading Edge." *Experiments in Fluids* 53: 1915-27.

[6] Bader, P., and Sanz, W. 2016. "On the Setup of a Test Bench for Predicting Laminar-to-Turbulent Transition on a Flat Plate." *Journal of Energy and Power Engineering* 10 (7): 411-24.

[7] Bader, P., Sanz, W., Peterleithner, J., Woisetschläger, J., Heitmeir, F., Meile, W., and Brenn, G. 2016. "Detecting Transition on Flat Plate Flow with Laser Interferometric Vibrometry (LIV)." In *Proceedings of ASME Turbo Expo 2016: Turbine Technical Conference and Exposition,*

Seoul, South Korea.

[8] Walters, D. K., and Cokljat, D. 2008. "A Three-Equation Eddy-Viscosity Model for Reynolds-Averaged Navier-Stokes Simulations of Transitional Flow." *Journal of Fluids Engineering* 130 (12): 121401.

[9] Langtry, R. B. 2006. "A Correlation-Based Transition Model Using Local Variables for Unstructured Parallelized CFD Codes." *AIAA Journal*.

[10] Wilcox, D. C. 1998. *Turbulence Modeling for CFD.* DCW Industries, 2nd edition.

[11] Coupland. 1990. "Flat Plate Transitional Boundary Layers." University lecture, University of Manchester.

[12] Persico, G., Gaetani, P., and Guardone, A. 2005. "Design and Analysis of New Concept Fast-Response Pressure Probes." *Measurement Science and Technology* 16 (9): 1741.

[13] Camp, T. R., and Shin, H. W. 1994. "Turbulence Intensity and Length Scale Measurements in Multistage Compressors." In ASME 1994 International Gas Turbine and Aeroengine Congress and Exposition. American Society of Mechanical Engineers.

[14] Persico, G., Gaetani, P., and Paradiso, B. 2008. "Estimation of Turbulence by Single-Sensor Pressure Probes." In *Proceedings of the XIX Biannual Symposium on Measuring Techniques in Turbomachinery Transonic and Supersonic Flow in Cascades and Turbomachines*, 7-8.

[15] Wallace, J. D., and Davis, M. R. D. 1996. "Turbulence Measurements with a Calibrated Pitot Mounted Pressure Transducer." In *Proceeding of the 13th Symposium on Measuring Techniques in Turbomachinery,* Zürich.

[16] Axelsson, L. U., and George, W. K. 2008. "Spectral Analysis of the Flow in an Intermediate Turbine Duct." In *ASME Turbo Expo 2008: Power for Land, Sea, and Air, American Society of Mechanical Engineers,* 1419-26.

[17] Pope, S. B. 2001. *Turbulent Flows*. Cambridge University Press.

[18] Schlichting, H., and Gersten, K. 1968. *Boundary-Layer Theory*. McGraw-Hill, 8th edition.

[19] Farabee, T. M. 1986. *An Experimental Investigation of Wall Pressure Fluctuations beneath Non-equilibrium Turbulent Flows.* Technical Report, DTIC Document.

[20] Barrett, R. 2000. "Transition Detection for Laminar Flow Aircraft Using Microphones beneath the Surface of Laser Drilled Suction Panels." Proceedings of the Institution of Mechanical Engineers, Part G: Journal of Aerospace Engineering, *SAGE Journals* 214 (3): 143-55.

[21] Stotz, S., Wakelam, C., Guendogdu, Y., and Niehuis, R. 2014. "Detection of Boundary Layer Transition on a Low Pressure Turbine Airfoil without Separation Using a Preston Tube and Hot Film Anemometry." In *Proceedings of 15th International Symposium on Transport Phenomena and Dynamics of Rotating Machinery (ISROMAC-15),* Honolulu, 24-8.